Hindawi
Geofluids
Volume 2023, Article ID 2307881, 17 pages
https://doi.org/10.1155/2023/2307881

Research Article

Experimental Study on the Effect of Coarse Grain Content on the Dilatancy and Particle Breakage Characteristics of Coarse-Grained Soils

Jun Du,[1] **Zhiming Xiong**,[2] **Xinggang Shen**,[1] **and Chenchen Li**[1]

[1]*College of Architecture and Civil Engineering, Kunming University, Kunming, 650214 Yunnan, China*
[2]*Faculty of Public Safety and Emergency Management, Kunming University of Science and Technology, Kunming, 650093 Yunnan, China*

Correspondence should be addressed to Jun Du; dujun0605@126.com

Received 8 August 2022; Revised 3 November 2022; Accepted 31 March 2023; Published 25 April 2023

Academic Editor: Yi Xue

The dilatancy deformation and particle breakage effects of coarse-grained soil have a significant influence on the safety and stability of high earth and rock-fill dams. To study the shear deformation and particle breakage characteristics of coarse-grained soil, four groups of soil sample with different coarse grain contents were to conduct consolidated drained triaxial compression tests by DJSZ-150 large-scale triaxial compression test machine. The results showed that the volume of coarse-grained soil changes significantly under deviation stress. The soil samples underwent positive dilatancy under the confining pressures of 200 kPa and 400 kPa but negative dilatancy under the confining pressures of 600 kPa and 800 kPa. When increasing the coarse grain contents in the soil sample under the same confining pressure, the positive dilatancy was more significant. A three-parameter dilatancy equation of coarse-grained soil considering confining pressure was established, in which the parameter $L = 4$ could serve as a criterion for whether the coarse-grained soil underwent positive dilatancy. Under the load, the coarse-grained soil showed three particle breakage modes: abrasion, attrition, and fracture. The coarse-grained soil particle size distribution before and after breakage conformed to the fractal characteristics, and the particle breakage rate increased significantly with larger soil particle size fractal dimension differences before and after the test. The coarse grain content and the confining pressure are two important factors affecting the mechanical properties of coarse-grained soil, and they control the shear deformation of soil.

1. Introduction

Earth and rock-fill dams have become the main form of high dams due to their adaptability to different site conditions, in situ material extraction, structural simplicity, and ease of construction [1]. Coarse-grained soils widely used as filling for dam construction are a class of broad-gradation gravel soils with widely varying grain sizes, and particle breakage under high stress is very frequent. Particle breakage causes significant deformation of the dam, which in turn leads to surface layer cracking that increases the seepage at the adjacent positions. These issues jeopardize dam safety, which makes them the current hot topics and challenges in earth and rock-fill dam engineering and construction. Therefore, studying the deformation characteristics and particle breakage effect of coarse-grained soil for dam construction is important to control the deformation of high dams.

Unlike common continuum materials, the strength and deformation properties of coarse-grained soils are significantly influenced by their gradation composition [2–4]. Due to the different proportions of coarse and fine particles, the structural characteristics of coarse-grained soils are significantly different, and their deformation failure resistance capacities vary. In coarse-grained soils, the coarse particles are closely arranged and in contact with each other to serve as the skeleton, while the fine particles fill randomly in the pores. Thus, the pore structure variation in the soil is the main factor affecting the mechanical properties of coarse-

grained soils [5–7]. Research has shown that the mechanical properties and deformation failure characteristics of coarse-grained soils are not only dependent on the fine-grained phase [8] but also prominently influenced by the content, spatial distribution, morphology, particle size composition, and other constitutive features of the aggregate [9–12]. On the one hand, coarse-grained soils have very complex particle compositions [13–15] and constantly changing contact relationships between particles in the spatial domain due to the different contents of coarse and fine particles [16]. As a result, the soil mass bearing capacity and deformation failure change accordingly. On the other hand, although coarse-grained soils mainly undergo shear yielding in terms of mechanical properties, they are highly susceptible to particle breakage under load [17–20], and the soil shear deformation has obvious dilatancy characteristics [21–23]. There granular material mechanical behaviors manifested in soil shear deformation render the shear strength characteristics of coarse-grained soils highly complicated. Tang et al. [24] found that the internal friction angle and cohesion of coarse-grained soils tended to increase and then decrease with the increase of coarse grain content, and the porosity changed accordingly, which in turn caused differences in the dilatancy characteristics of soils with different coarse grain contents. After comparing the current particle size distribution and the limit particle size distribution of soils, Hardin [25] proposed the particle breakage rate to theoretically describe the breakage effect of soil particles, which has been adopted extensively by researchers. Alaei and Mahboubi [26] pointed out that particle breakage directly changed the soil particle gradation and affected a series of physical properties such as soil particle aggregate structure, the occlusion degree, and the interparticle friction, thus changing the deformation and shear strength of the soil mass. Huang et al. [27] analyzed the effect mechanism of particle breakage on the mechanical properties of coarse-grained soils such as rock-fill materials and elucidated the different methods of rock-fill material particle breakage measurement and the effect of particle breakage on their strength and dilatancy. Liu et al. [28] conducted triaxial tests to study the variations of rock-fill material particle breakage and dilatancy under different void ratios, and the results provide guidance for further understanding of the particle breakage characteristics of rock-fill materials.

Although the strength and deformation characteristics of coarse-grained soil have been analyzed in-depth, the intrinsic action mechanism of soil particles and shear deformation mechanism of soil mass are not yet clear because the structure characteristics of coarse-grained soil are extremely complex. Thus, it is urgent to study the mechanical response characteristics and particle breakage effect of soil mass. This study carried out large-scale triaxial compression tests on coarse-grained soil considering different coarse grain contents and different confining pressure conditions to analyze their shear yield deformation characteristics and change law of particle breakage. Applicability of quadratic function between axial strain ε_1^2 and lateral strain ε_3 is convinced for coarse-grained soil, and an experiential dilatancy criterion of coarse-grained soil considering confining pressure is established. The difference of soil fractal dimension before and after particle breakage is used to quantitatively characterize the breakage law of soil particles. The research results have strong scientific guiding significance for in-depth understanding of the mechanical properties of dam materials and have certain technical support for stress-strain analysis and stability calculation of high earth and rock-fill dams.

2. Triaxial Compression Test on Coarse-Grained Soil

2.1. Test Material and Gradation Design. The test soil samples were collected from the dam rock-fill material of Daqiaopo reservoir in Lincang, Yunnan. The soil material was blasted and processed from gravel, whose parent rock was weakly weathered granite. The rock had an average saturated uniaxial compressive strength of 50 MPa, a softening coefficient of 0.79, and a specific gravity of 2.70. In order to meet the requirements of the maximum particle size of 60mm when preparing soil samples by indoor triaxial compression testing machine. According to the Standard for Geotechnical Testing Methods (GB/T50123-2019), the gradation of the soils on site was scaled down based on the equivalent replacement method by Equation (1), and the maximum particle size was 60 mm. The dividing particle size of coarse and fine particles was 5 mm [29], i.e., particles below 5 mm were fine particles, and those beyond 5 mm were coarse particles. The coarse grain content was expressed as P_5. This study was conducted to analyze the effect of changes in the structural characteristics of coarse-grained soil caused by different coarse grain contents on their deformation characteristics. After test soil gradation scaling, four test gradations were designed according to the different coarse grain contents P_5, as shown in Table 1, where the coarse grain contents P_5 are 30%, 45%, 60%, and 75%. The gradation accumulation curves of soil samples with different coarse grain contents are shown in Figure 1.

$$P_{5i} = P_{05i} \cdot \frac{P_5}{P_5 - P_0}, \tag{1}$$

where P_5 is the coarse grain content (%), P_{5i} is the content of a particle group with a particle size greater than 5 mm after scaling (%), P_{05i} is the content of a particle group with a particle size greater than 5 mm before scaling (%), and P_0 is the percentage of particle mass with a particle size greater than 60 mm.

2.2. Test Apparatus and Test Program. The triaxial compression tests were conducted on a DJSZ-150 large-scale coarse-grained soil dynamic and static triaxial testing machine. The testing machine consists of five parts: the confining pressure servo system, the dynamic and static loading system, the pore pressure measurement system, the volumetric variation measurement system, and the data collection system. Other than the conventional triaxial tests, the testing machine could also facilitate different stress path loading tests. The specimen size was $\Phi 300 \times 600$ mm. The maximum axial

Table 1: Particle size compositions of coarse-grained soils with different coarse grain contents.

Gradation characteristics	Content (%) of each particle group with different particle sizes (mm)						
	<2	2~5	5~10	10~20	20~40	40~60	>60
Site gradation	8.31	4.04	8.58	15.22	24.37	18.66	20.82
Scaled gradation	8.31	4.04	11.25	19.96	31.97	24.47	—
$P_5 = 30\%$	47.05	22.95	3.86	6.83	10.94	8.37	—
$P_5 = 45\%$	36.96	18.04	5.79	10.24	16.41	12.56	—
$P_5 = 60\%$	26.88	13.12	7.72	13.66	21.88	16.74	—
$P_5 = 75\%$	16.80	8.20	9.65	17.07	27.35	20.93	—

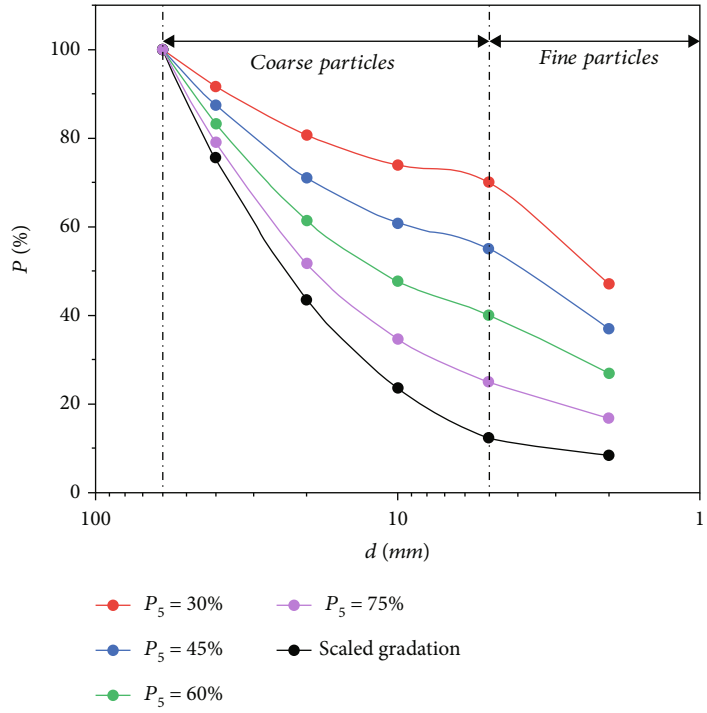

Figure 1: Grading curve of coarse-grained soils.

force of the testing machine could reach 1500 kN, and the maximum confining pressure could reach 3.0 MPa.

The coarse-grained soil samples with 30%, 45%, 60%, and 75% coarse grain contents were conducted to consolidated drained triaxial compression tests using the DJSZ-150 coarse-grained soil triaxial testing machine. The density of the soil samples was 2.12 g/cm^3, and the natural water content was 4.2%. First, the test soil material was air-dried, and then the particles were sieved. Finally, according to the test grading composition, the soil of different particle groups were weighed. The soil material was filled into the sample cylinder with five layers; the filling height of each layer should be strictly controlled. The test operation was performed in accordance with the Standard for Geotechnical Testing Methods (GB/T50123-2019). Strain control method was adopted for the test loading, and the shear rate of the triaxial compression test was set as 1 mm/min. When the compressive deformation of the sample reached 15% of the strain, it was considered as failure. The confining pressures were designed as 200 kPa, 400 kPa, 600 kPa, and 800 kPa. After the tests, soil samples with shear failures were air-dried, and their particle size composition was determined. The testing machine and test process are shown in Figure 2.

3. Analysis of Coarse-Grained Soil Dilatancy Characteristics

3.1. Volumetric Deformation Characteristics. Soils undergoing shear deformation produce not only shape changes but also volumetric changes. The soil volume expansion and contraction caused by shear stress are collectively referred to as soil dilatancy properties. In the triaxial compression tests, the volumetric deformation of the soil samples was obtained by measuring the water discharges. The volumetric strain for the negative dilatancy of the soil samples was set to be positive, and the volumetric strain for the positive dilatancy was set to be negative. The volumetric strain ε_v versus axial strain ε_1 curves of the soil samples with different coarse

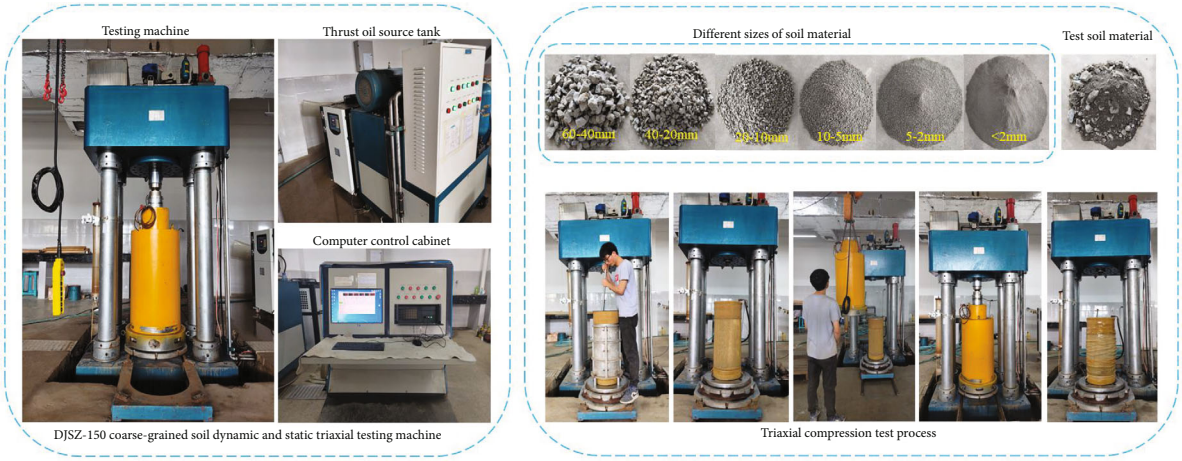

Figure 2: Triaxial compression test for coarse-grained soil.

grain contents and under the confining pressures of 200 kPa, 400 kPa, 600 kPa, and 800 kPa are shown in Figure 3.

According to Figure 3, the soil samples with different coarse grain contents show the characteristics of negative dilatancy before positive dilatancy under the confining pressures of 200 kPa and 400 kPa. Additionally, lower confining pressures lead to more significant positive dilatancy of the soil samples. Under the same confining pressure, the axial strain corresponding to the positive dilatancy decreases as the coarse grain content increases, and the final dilatancy volumetric strain increases. Therefore, soil samples with higher coarse grain contents are more likely to produce positive dilatancy and more obvious volume expansion characteristics. As an example, the axial strains corresponding to the positive dilatancy of soil samples with 30%, 45%, 60%, and 75% coarse grain contents were 9.5%, 8.5%, 7.5%, and 6%, and the final volumetric strains were -0.73%, -1.56%, -1.79%, and -2.36% under the confining pressure of 200 kPa. The soil samples with different coarse grain contents show the characteristics of negative dilatancy under the confining pressures of 600 kPa and 800 kPa. In addition, higher confining pressures lead to more significant negative dilatancy of the soil samples. Under the same confining pressure, the final negative dilatancy volumetric strain decreases as the coarse grain content increases. For example, the volumetric strains for the negative dilatancy of soil samples with 30%, 45%, 60%, and 75% coarse grain contents were 2.05%, 1.75%, 1.46%, and 1.25% under the confining pressure of 800 kPa. Therefore, the confining pressure and the coarse grain content are two important factors affecting the dilatancy of coarse-grained soils. Specifically, the soil samples underwent positive dilatancy under low confining pressures but negative dilatancy under high confining pressures. Soil samples with higher coarse grain contents are more likely to produce positive dilatancy and less likely to produce negative dilatancy.

The volumetric strain of the soil samples undergoing shear deformation can be expressed as

$$\varepsilon_v = 2\varepsilon_3 + \varepsilon_1, \tag{2}$$

where ε_v is the volumetric strain of the soil sample, ε_3 is the lateral strain of the soil sample, and ε_1 is the axial strain of the soil sample.

The lateral strain ε_3 of the soil sample can be calculated with Equation (2):

$$\varepsilon_3 = \frac{1}{2}(\varepsilon_v - \varepsilon_1). \tag{3}$$

The tangent Poisson's ratio ν_t of the soil samples undergoing shear deformation can be calculated with the lateral strain ε_3 and the axial strain ε_1. The tangent Poisson's ratio ν_t versus axial strain ε_1 curves of the soil samples with different coarse grain contents and under the confining pressures of 200 kPa, 400 kPa, 600 kPa, and 800 kPa are shown in Figure 4.

According to Figure 4, the initial tangent Poisson's ratio ν_i of the soil samples tends to zero. As the axial strain ε_1 increases, the tangent Poisson's ratio ν_t of the soil samples increases first before stabilizing. As the confining pressure increases, the increase in the tangent Poisson's ratio ν_t of soil samples with the same coarse grain content decelerates. The volumetric changes of coarse-grained soil in the triaxial compression tests can be analyzed based on the tangent Poisson's ratio ν_t. When $\varepsilon_v = 0$, i.e., no expansion or contraction of the soil samples, we have $\varepsilon_3 = -0.5\varepsilon_1$ according to Equation (2). Then, $\nu_t = |d\varepsilon_3/d\varepsilon_1| = 0.5$. Therefore, the soil samples produce positive dilatancy when the tangent Poisson's ratio $\nu_t > 0.5$; the soil samples produce negative dilatancy when the tangent Poisson's ratio $\nu_t < 0.5$. Thus, under lower confining pressure, the tangent Poisson's ratio of the soil samples increases faster, and the soil samples are more likely to produce dilatancy deformation. The horizontal asymptote of the tangent Poisson's ratio ν_t curve of the soil samples was defined as the Poisson's ratio for their failure. If the Poisson's ratio $\nu_{tf} < 0.5$ at the time of soil sample failure, and since $\nu_t < \nu_{tf}$, the soil samples will not produce positive dilatancy. According to Figure 4, under the confining pressures of 200 kPa and 400 kPa, the Poisson's ratio $\nu_{tf} > 0.5$ at the time of soil sample failure, and the soil

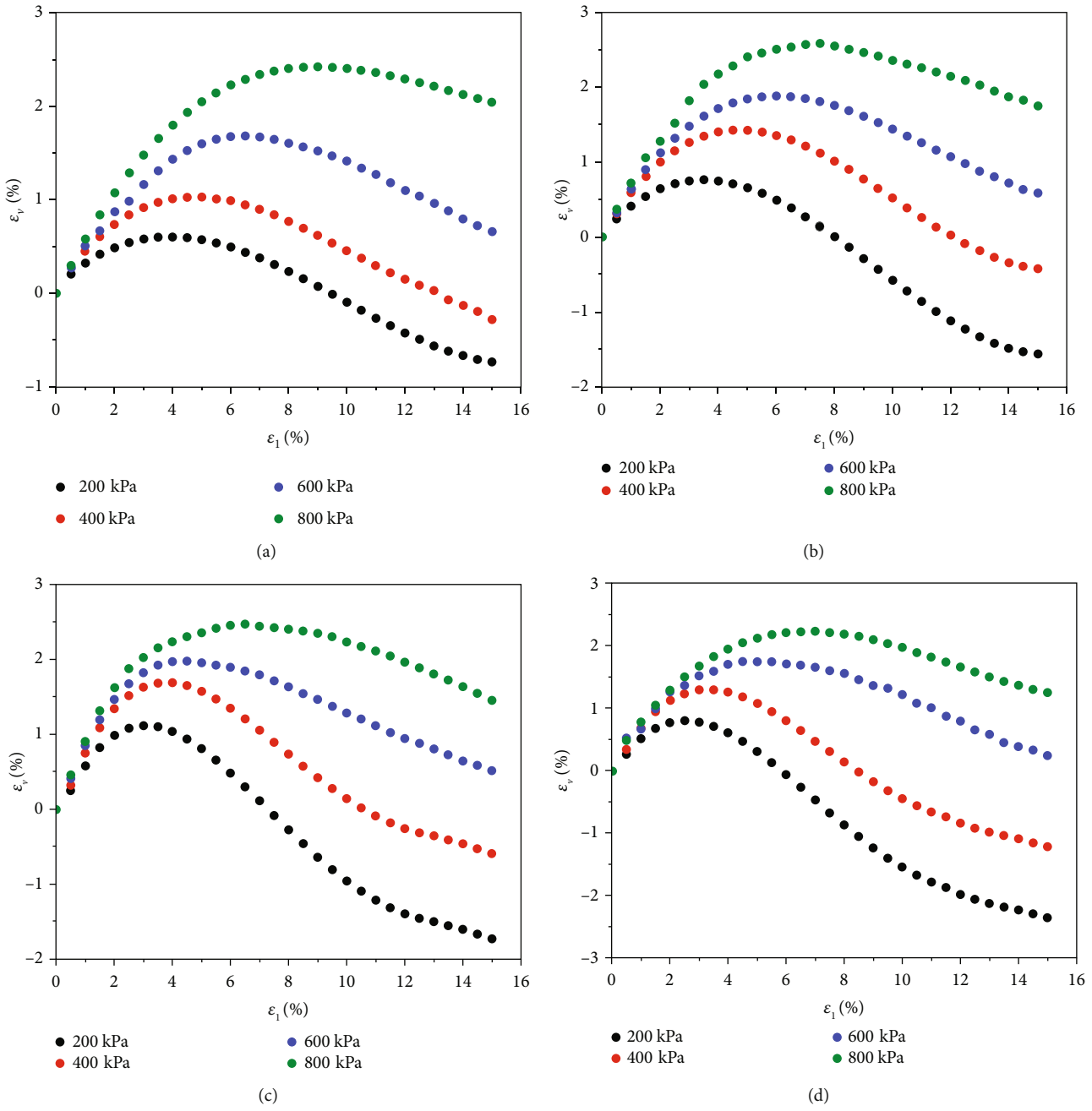

FIGURE 3: The volumetric strain ε_v versus axial strain ε_1 curves: (a) $P_5 = 30\%$; (b) $P_5 = 45\%$; (c) $P_5 = 60\%$; (d) $P_5 = 75\%$.

samples undergo positive dilatancy deformation failure, whereas under the confining pressures of 600 kPa and 800 kPa, the Poisson's ratio $\nu_{tf} < 0.5$ at the time of soil sample failure, and the soil samples undergo negative dilatancy deformation failure.

3.2. Dilatancy Deformation Mechanism of Coarse-Grained Soil. The dilatancy deformation in coarse-grained soil is mainly due to their structural properties. With a binary composite structure of soil and rock, the resistance of coarse-grained soil against the deformation induced by the external force is significantly affected by their coarse grain contents. As the coarse grain content gradually increases, hollow structures appear between the rocks, and the soil samples become less dense. At the initial stage of shear deformation, the coarse and fine particles in the soil samples are closely packed to reach a high density, thus manifesting volumetric contraction. As the shear stress increases, the coarse particle occlusion in the soil samples is gradually enhanced to obtain more shear space for the coarse particles. If the confining pressure is too low to limit the rotation and tumbling of coarse particles in the soil samples, the internal pore volume will increase continuously, leading to volumetric expansion. If the confining pressure is high enough to

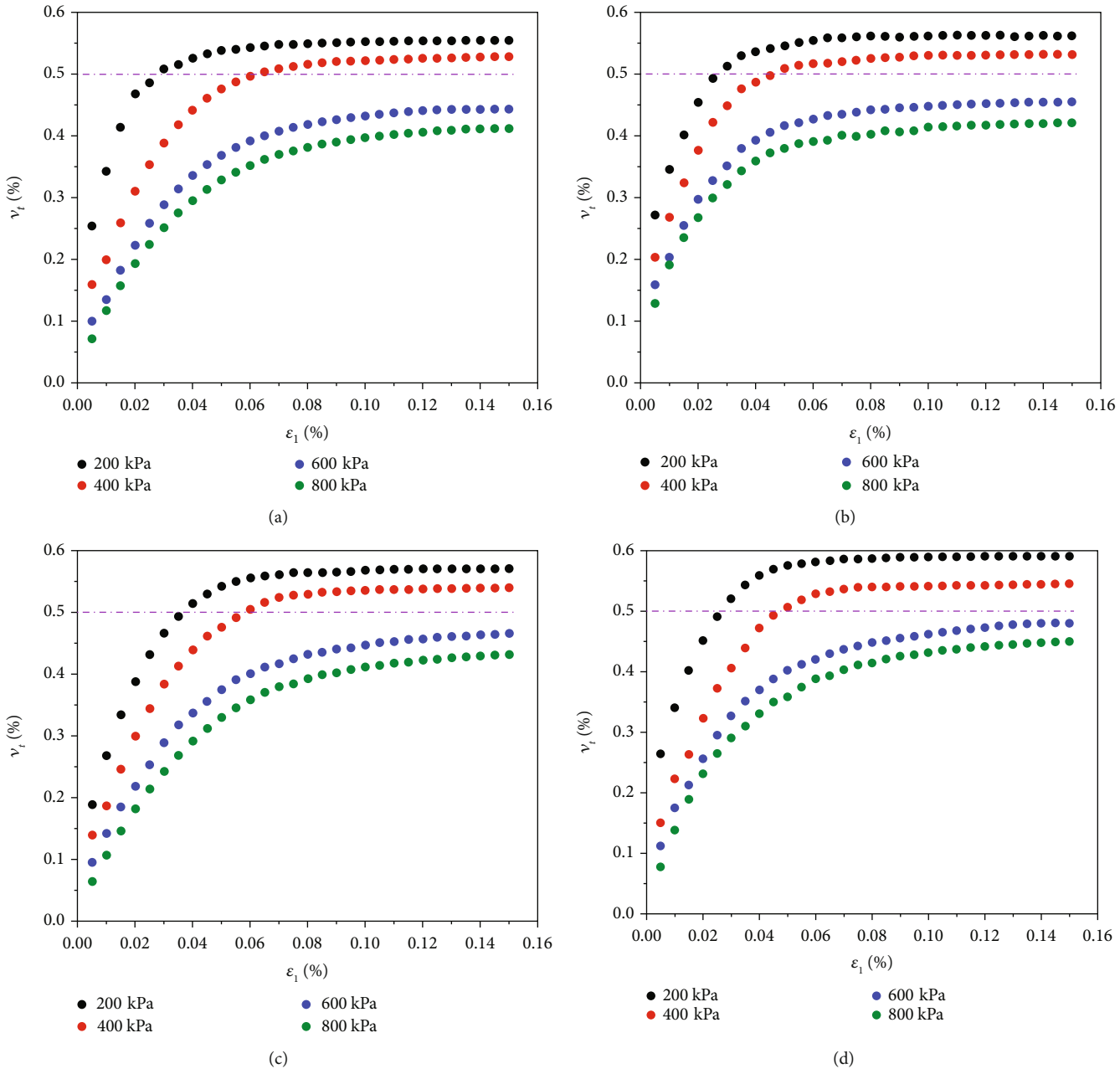

Figure 4: Tangent Poisson's ratio ν_t versus axial strain ε_1: (a) $P_5 = 30\%$; (b) $P_5 = 45\%$; (c) $P_5 = 60\%$; (d) $P_5 = 75\%$.

effectively inhibit the extrusion and occlusion between coarse particles, the coarse particles break due to stress concentration. The small particles from the fracture fill in the pores and reduce the pore volume of the soil samples, leading to volumetric contraction. However, the two states above are different. The former shows rapidly increasing shear stress within the soil samples due to the close occlusion between coarse particles. The latter shows higher soil sample density due to the fine particles filling the pores. With the continuous development of shear deformation, the principal stress difference within the soil samples gradually increases, as does the shear stress. As the shear stress exceeds the limit shear strength, the soil samples undergo shear failure.

3.3. Coarse-Grained Soil Dilatancy Model. To characterize the volumetric strain variation during shear deformation of coarse-grained soil, scholars have developed mathematical models of lateral strain ε_3 and axial strain ε_1 in soils. Liu et al. [30] established an exponential relationship between the lateral strain ε_3 and the axial strain ε_1 as follows:

$$\varepsilon_3 = \lambda\left(e^{\mu\varepsilon_1} - 1\right), \tag{4}$$

where λ and μ are the fitting parameters.

Zhang and Zhang [31] established the relationship between the lateral strain ε_3 and the axial strain ε_1 using a

parabolic equation:

$$\varepsilon_3 = \alpha\varepsilon_1^2 + \beta\varepsilon_1, \tag{5}$$

where α and β are the fitting parameters.

Xie et al. [32] simplified the relationship between axial and lateral strains as a straight line with a constant term of zero:

$$\varepsilon_3 = \alpha\varepsilon_1. \tag{6}$$

Although Equations (4), (5), and (6) characterize the relationship between axial strain ε_1 and lateral strain ε_3 to some extent, the nonlinear variation characteristics of the tangent Poisson's ratio of the soil mass are not well-reflected. Therefore, the relationship between axial strain ε_1 and lateral strain ε_3 is redefined in this study as follows:

$$\varepsilon_1^2 = L\varepsilon_3^2 + T\varepsilon_3, \tag{7}$$

where L and T are the fitting parameters.

The fitted relationship between ε_1^2 and ε_3 based on Equation (7) for soil samples with 60% coarse grain under different confining pressures is presented in Figure 5, and similar relationships are found for other soil samples. Judging from the correlation coefficients in Figure 5, Equation (7) can accurately describe the relationship between the axial strain ε_1 and the lateral strain ε_3 of the soil samples.

According to the fitting relationship in Figure 5, the parameters L and T show a trend of gradually increasing with the increase of the confining pressure in soil samples with the same coarse grain content and different confining pressures. The parameter T can be expressed as

$$T = G + F\lg\left(\frac{\sigma_3}{p_a}\right), \tag{8}$$

where σ_3 is the confining pressure (kPa), p_a is the standard atmospheric pressure (100 kPa), G and F are the fitting parameters, which can be obtained by linear fitting, as shown in Figure 6.

Based on the experimental data and Equations (7) and (8), the fitting parameters L, T, G, and F for soil samples with different coarse grain contents under the confining pressures of 200 kPa, 400 kPa, 600 kPa, and 800 kPa are shown in Table 2.

The mathematical solution of Equation (7) yields

$$\varepsilon_3 = \frac{T - \sqrt{T^2 + 4L\varepsilon_1^2}}{2L}. \tag{9}$$

The tangent Poisson's ratio ν_t of the soil samples can be obtained by finding the derivative of Equation (9):

$$\nu_t = \frac{d\varepsilon_3}{d\varepsilon_1} = \frac{\varepsilon_1}{\sqrt{L\varepsilon_1^2 + 0.25T^2}} = \frac{1}{\sqrt{L + ((G + F\lg(\sigma_3/p_a))/2\varepsilon_1)^2}}. \tag{10}$$

According to Equations (2), (8), and (9), the volumetric strain ε_v of the soil samples can be expressed as

$$\varepsilon_v = 2\varepsilon_3 + \varepsilon_1 = \varepsilon_1 + \frac{\left(T - \sqrt{T^2 + 4L\varepsilon_1^2}\right)}{L} = \varepsilon_1 + \frac{\left[G + F\lg(\sigma_3/p_a) - \sqrt{(G + F\lg(\sigma_3/p_a))^2 + 4L\varepsilon_1^2}\right]}{L}. \tag{11}$$

Thus, the tangent Poisson's ratio and volumetric strain of the soil samples with the coarse grain content of 60%, as an example, can be calculated with Equations (10) and (11), as shown in Figure 7. According to the comparison with the test results, the model calculation results have little derivation from the test results. The same pattern of comparison can be found in other soil samples. Therefore, the applicability of the quadratic function of axial strain ${\varepsilon_1}^2$ and lateral strain ε_3 in the shear deformation of coarse-grained soil is verified. In the meantime, Equations (10) and (11) can also objectively characterize the tangent Poisson's ratio and volumetric strain of the soil samples.

Further analysis of Figure 7(b) shows that the tangent Poisson's ratio ν_t of the soil mass gradually tends to a constant with the increase of axial strain during the shear deformation of coarse-grained soils. According to Equation (10), as the axial strain ε_1 tends to infinity, we have

$$\lim_{\varepsilon_1 \longrightarrow \infty} \nu_t = \frac{1}{\sqrt{L}}. \tag{12}$$

Equation (12) represents the horizontal asymptote of the soil sample tangent Poisson's ratio curve when $\nu_t = 1/\sqrt{L}$, which also indicates that the soil sample tangent Poisson's ratio should always fall below $1/\sqrt{L}$ during the shear deformation. If $1/\sqrt{L} \le 0.5$, the tangent Poisson's ratio ν_t of the soil samples will always fall below 0.5, indicating that the soil samples will not undergo positive dilatancy deformation. At this point, the soil sample parameter $L = 4$ can serve as an important parameter to analyze whether the soil sample undergoes positive dilatancy deformation or not. That is, with $L > 4$, no positive dilatancy occurs in the soil sample; with $L < 4$, positive dilatancy occurs in the soil sample. Therefore, according to the statistical results of parameter L in Table 2, L gradually decreases with the increase of coarse grain content or the decrease of confining pressure, indicating that the soil samples with lower confining pressure or higher coarse grain contents are more likely to produce positive dilatancy deformation. This also suggests that the confining pressure and the coarse grain content are two important factors affecting the dilatancy of coarse-grained soils.

In summary, the parameter L in the proposed coarse-grained soil empirical equation of dilatancy criterion can characterize the dilatancy properties of the soil samples. Coarse-grained soil with higher particle irregularity, higher angularity, higher coarse grain content, and higher density

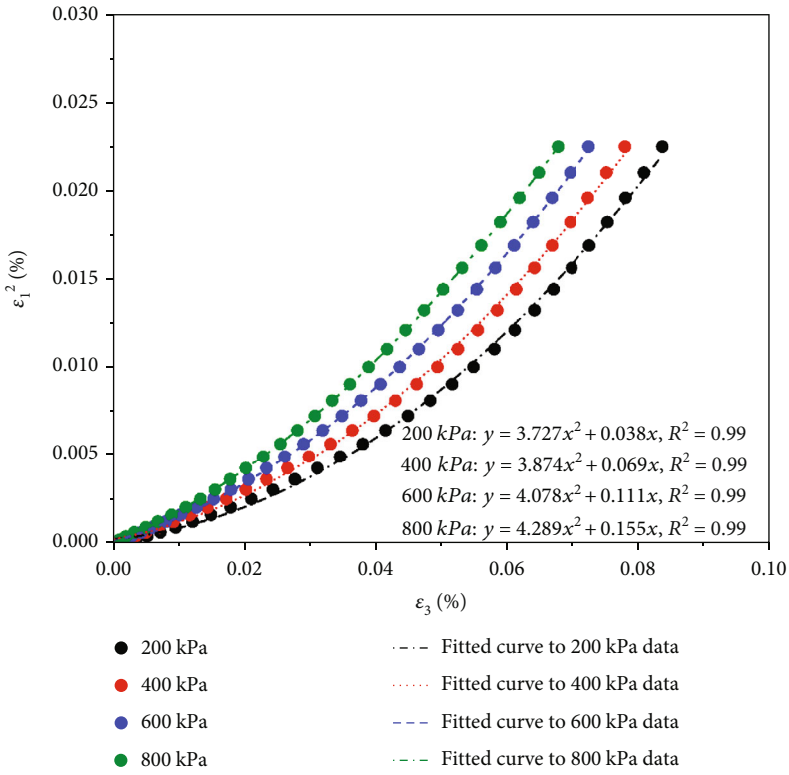

Figure 5: Fitting relationship between ε_1^2 and ε_3.

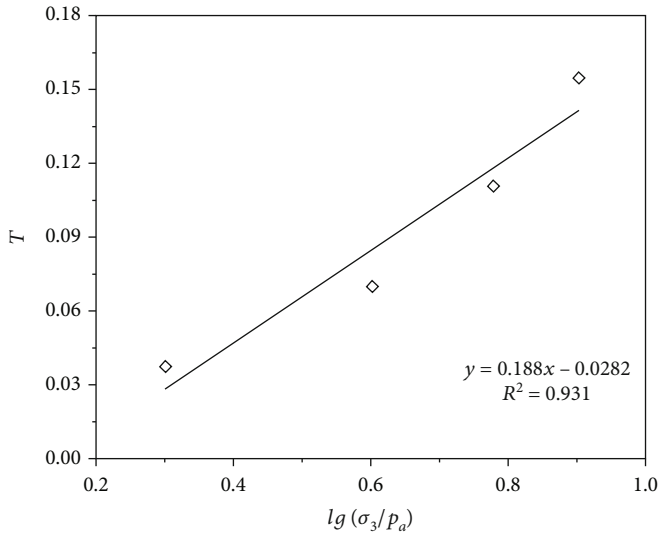

Figure 6: Fitted curve between parameter T and $\lg(\sigma_3/p_a)$.

Table 2: Statistical results of fitting parameters.

P_5 (%)	L				T				G	F
	$\sigma_3 = 200$ kPa	$\sigma_3 = 400$ kPa	$\sigma_3 = 600$ kPa	$\sigma_3 = 800$ kPa	$\sigma_3 = 200$ kPa	$\sigma_3 = 400$ kPa	$\sigma_3 = 600$ kPa	$\sigma_3 = 800$ kPa		
30	3.807	3.953	4.152	4.325	0.049	0.074	0.119	0.151	0.017	0.011
45	3.786	3.916	4.106	4.303	0.056	0.094	0.127	0.165	0.018	0.021
60	3.727	3.874	4.078	4.289	0.038	0.069	0.111	0.155	0.019	-0.005
75	3.691	3.822	4.033	4.241	0.021	0.051	0.117	0.144	0.022	-0.026

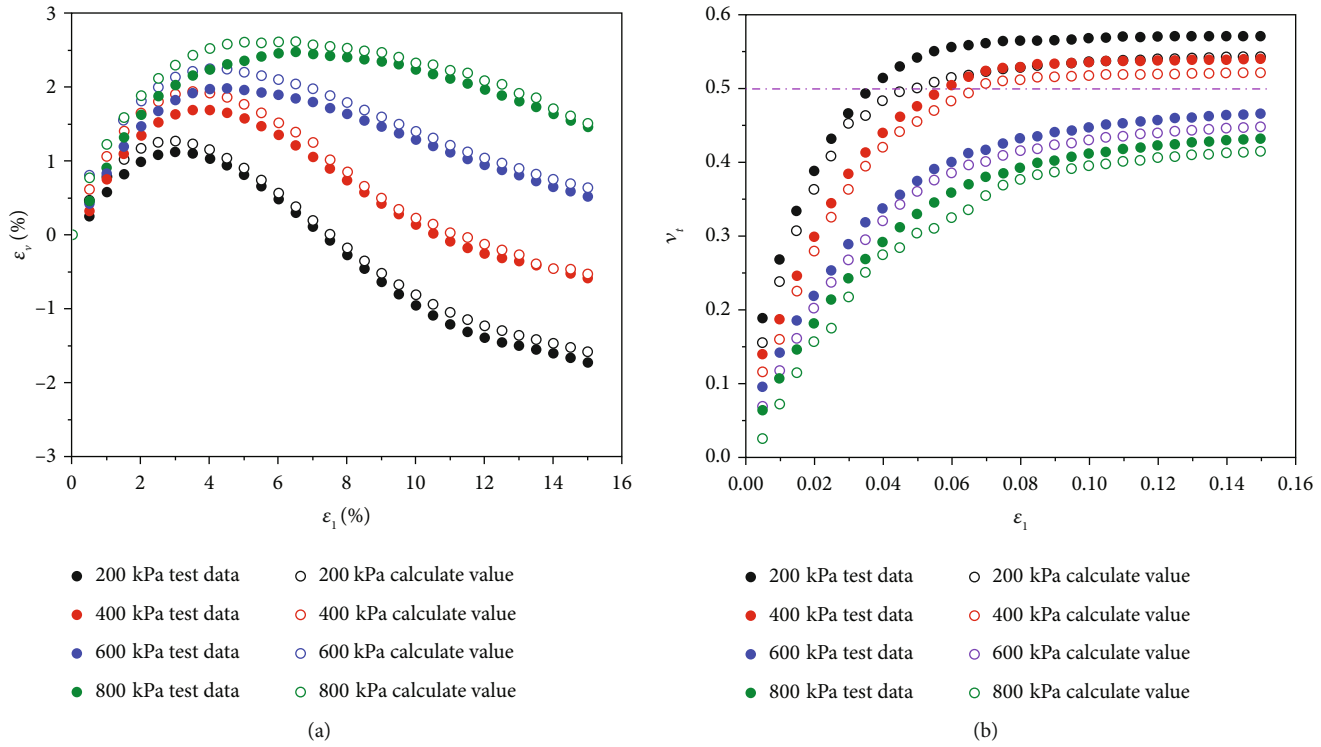

Figure 7: Comparison between model calculation results and test results: (a) volumetric strain versus axial strain; (b) tangent Poisson's ratio versus axial strain.

are prone to positive dilatancy under external load. Meanwhile, the corresponding soil sample parameter L should fall below 4. Therefore, parameter L can be used to reflect the particle size distribution, particle shape, and compaction degree of coarse-grained soils.

4. Particle Breakage Characteristic Analysis

4.1. Particle Breakage Characteristics. In the triaxial compression tests, the skeleton of the coarse-grained soils was formed based on the interparticle contact in the form of mutual occlusion and friction and the stacked aggregate structure. With the continuous increase of external load, slipping and flipping occur between the particles for larger shear space, and the contact force of mutual occlusion between the particles further increases. Due to the stress concentration, localized particle breakage occurs in the stressed soil aggregate. Coarse-grained soils often produce three types of particle breakage under load, i.e., abrasion, attrition, and fracture, as shown in Figure 8.

Particle fracture produces many subparticles of similar size. Particle attrition produces particles of similar size to the original particles and many smaller particles. Particle abrasion causes the detachment of some fine particles from the original particles. Coarse-grained soils produce shear deformation under deviatoric stress. At the beginning of shear deformation, the axial pressure gradually increases, the particles first undergo mutual extrusion and occlusion, and the irregular rock particles in contact with each other undergo abrasion under contact friction. With the continuous development of shear deformation, the rock particles slipping over the adjacent particles undergo attrition as part of their irregular angles are ground off. As the shear stress gradually increases and approaches the peak, the rock particles undergo fracture due to the stress concentration that exceeds their strength, forming subparticles with angularity.

4.2. Particle Breakage Rate. The current determination of particle breakage rate is mostly based on the quantitative statistics of the different soil sample particle size compositions before and after the tests. In this study, the particle breakage rate B_g defined by Marsal [33] is adopted to measure the degree of particle breakage, where B_g is the sum of the absolute mass differences of each particle size composition before and after the test, i.e.,

$$B_g = \sum \left| W_{ki} - W_{kf} \right|, \tag{13}$$

where W_{ki} is the mass fraction of a grain group on the soil sample gradation curve before the test, while W_{kf} is the mass fraction of a grain group on the soil sample gradation curve after the test.

The grain gradation of soil samples with different coarse grain contents after triaxial compression tests under different confining pressures is recorded and shown in Table 3.

According to Table 3, the soil samples with different coarse grain contents show different particle breakage rates in the triaxial compression tests. The particle breakage rate of the coarse-grained soils in the test was recorded, and the relationship between the breakage rate and the confining pressure variation was established, as shown in Figure 9.

Figure 8: Particle breakage modes: (a) abrasion; (b) attrition; (c) fracture.

Table 3: Results of coarse-grained soil particle breakage analysis after triaxial compression test.

P_5 (%)	σ_3 (kPa)	Content (%) of each particle group with different particle sizes (mm)						B_g (%)
		<2	2~5	5~10	10~20	20~40	40~60	
30	200	49.05	22.78	3.43	7.16	10.96	6.62	4.70
	400	49.88	22.58	3.32	7.24	10.82	6.16	6.48
	600	50.28	22.56	3.36	7.26	10.68	5.86	7.32
	800	51.05	22.47	3.33	6.98	10.89	5.28	8.30
45	200	40.13	17.72	6.34	10.16	15.51	10.14	7.44
	400	40.92	17.44	5.82	10.20	15.90	9.72	7.98
	600	41.86	17.16	5.79	10.12	15.83	9.24	9.80
	800	42.38	17.26	5.94	10.34	15.75	8.33	11.34
60	200	30.61	12.54	8.58	13.45	21.28	13.54	9.18
	400	31.58	12.84	8.13	13.86	20.72	12.87	10.62
	600	32.64	12.72	8.04	14.16	20.48	11.96	13.16
	800	34.13	12.84	7.88	14.79	19.48	10.88	17.08
75	200	20.68	8.46	10.60	16.14	26.82	17.30	10.18
	400	21.82	8.66	11.02	15.80	26.44	16.26	13.70
	600	22.04	8.98	11.96	15.88	25.24	15.90	16.66
	800	23.97	9.17	12.24	14.98	25.62	14.02	21.46

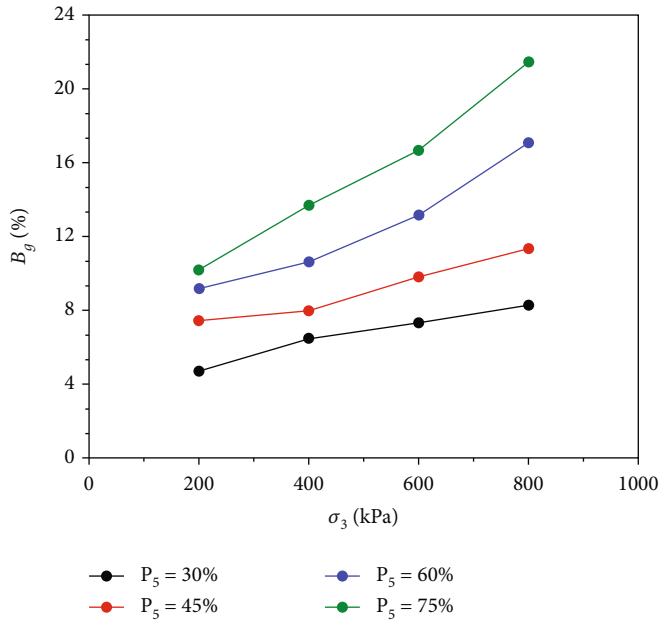

Figure 9: Relationship between particle breakage rate and confining pressure.

On the one hand, the coarse-grained soil particle breakage rate increases with the increase of the confining pressure under the same gradation conditions. The reason is that under the initial consolidation stress, the higher confining pressure for consolidation leads to the more adequate interparticle occlusion, and the particles are more likely to fracture when slipping under shear pressure. On the other hand, the coarse-grained soil particle breakage rate increases with the increase of coarse grain content under the same confining pressure. The reason is that under the same confining pressure, coarse-grained soils with higher coarse grain contents have more obvious interparticle occlusion and extrusion, and the irregular rock particles slipping over the adjacent particles are more likely to fracture during shear deformation.

4.3. Fractal Characteristics of Particle Breakage. Soil particles are broken under load and their gradation composition changes. The cumulative curve of particle gradation used to describe the composition of soil gradation cannot directly reflect the degree of fragmentation of soil. Fractal geometry is often used to describe irregular and disordered phenomena and behaviors in nature. It has been widely used in geotechnical studies, and fractal dimension has become an important index for investigating the physical and mechanical properties of geotechnical materials. In order to quantitatively analyze the change of soil particle fragmentation before and after the test, the fractal dimension of fractal theory is introduced to quantitatively calculate the change of soil gradation. According to the difference of soil fractal dimension before and after the test, the degree of soil particle fragmentation can be calculated directly. Zhang et al. [34] pointed out that the mass of soil grain groups could be easily obtained from sieving tests, and the mass-grain size fractal model could be used to characterize the grain group composition and gradation of coarse-grained soils, namely,

$$\frac{M(\delta < d_i)}{M_t} = \left[\frac{d_i}{d_m}\right]^{3-D}, \tag{14}$$

where d_i is the particle diameter, $M(\delta < d_i)$ is the mass of particles with diameters below d_i, M_t is the total mass of the particles, d_m is the maximum particle diameter, D is the fractal dimension.

Taking the logarithm of both sides of Equation (14) yields

$$\lg\left(\frac{M(\delta < d_i)}{M_t}\right) = (3 - D)\lg\left(\frac{d_i}{d_m}\right). \tag{15}$$

In Equation (15), $M(\delta < d_i)/M_t$ can be obtained by sieving test statistics. Then, the slope k of the $\lg(d_i/d_m) \sim \lg(M(\delta < d_i)/M_t)$ linear relationship can be obtained based on linear regression, i.e., the $3 - D$ in Equation (15). In turn, the fractal dimension can be found as follows:

$$D = 3 - k. \tag{16}$$

The relative contents of accumulated mass under the sieve $M(\delta < d_i)/M_t$ corresponding to different particle sizes were recorded, and the relationship between $M(\delta < d_i)/M_t$ and d_i/d_m was established in bi logarithm coordinates. The particle size fractal distribution curves of coarse-grained soils before and after the triaxial compression tests are plotted in Figure 10.

According to Figure 10, although the coarse and fine particle sizes of the test soil material differ greatly, the soil material particle size composition $\lg(M(\delta < d_i)/M_t)$ and $\lg(d_i/d_m)$ have good linear correlations before and after the tests. Thus, the particle size distribution after coarse-grained soil particle breakage under load conforms to the fractal distribution, and the particle size composition has a good fractal structure that satisfies the self-similarity law in terms of statistics. The statistics of soil fractal dimension before and after particle breakage are shown in Table 4.

Fractal dimension D is a quantitative indicator of coarse-grained soil particle size fractal distribution, and the magnitude of coarse-grained soil particle size changes before and after the triaxial compression tests characterizes the degree of particle breakage. As shown in Table 4, the fractal dimension of the coarse-grained soils after the tests is larger than that before the tests, and the fractal dimension differences before and after the tests increase with the increase of confining pressure under the same gradation conditions. To analyze the relationship between coarse-grained soil particle breakage rate and particle size fractal dimension, the relationship curves between the particle breakage rates and the particle size fractal dimension differences were established based on the results in Tables 3 and 4, as shown in Figure 11.

According to Figure 11, the particle size fractal dimension difference and the particle breakage rate of coarse-grained soils before and after the tests have a corresponding relationship. Specifically, a small fractal dimension difference leads to a low particle breakage rate, while larger fractal dimension differences lead to more significant particle breakage. Therefore, the magnitude of fractal dimension difference, like the particle breakage rate, can objectively characterize the particle breakage degree of coarse-grained soils during shear failure.

The relationship between the coarse-grained soil breakage fractal dimension and the confining pressure after triaxial compression tests is shown in Figure 12. With the same coarse grain content, the coarse-grained soil breakage fractal dimension after the tests gradually increases with the increase of confining pressure in soil samples. The reason is that the increased confining pressure inhibits the lateral deformation of the coarse-grained soil, and the occlusal contact force between the particles increases significantly. The stress concentration causes the irregular particles to fracture at their contact positions. The particle breakage becomes increasingly significant with the continuous increase of axial load. Meanwhile, the fine particle content in the soil samples gradually increases, as does the fractal dimension of the soil samples.

5. Discussion

Based on the analysis of dilatancy deformation and particle breakage effect of coarse-grained soil under triaxial compression test, it can be seen that coarse grain content and confining pressure are two important factors affecting the

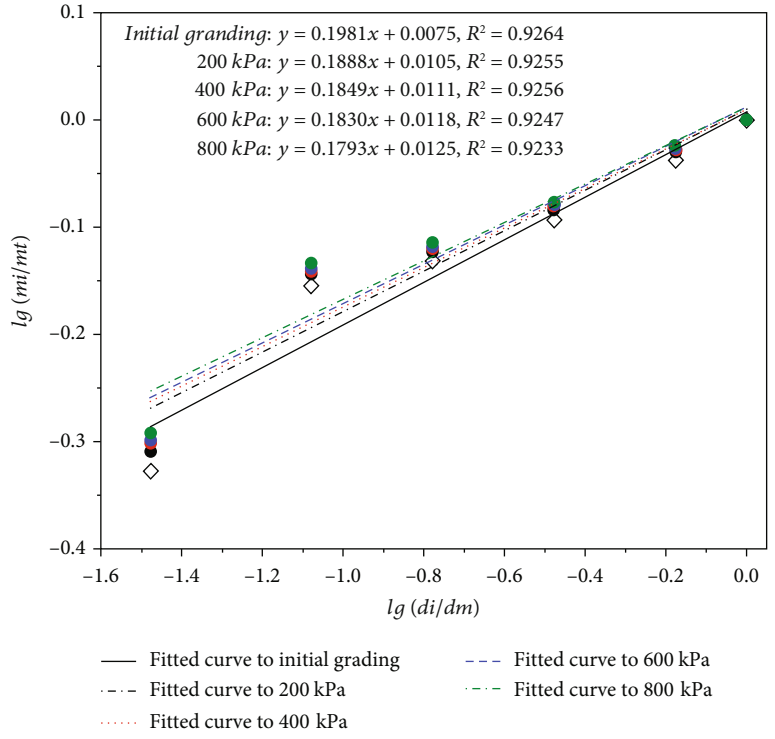

(a)

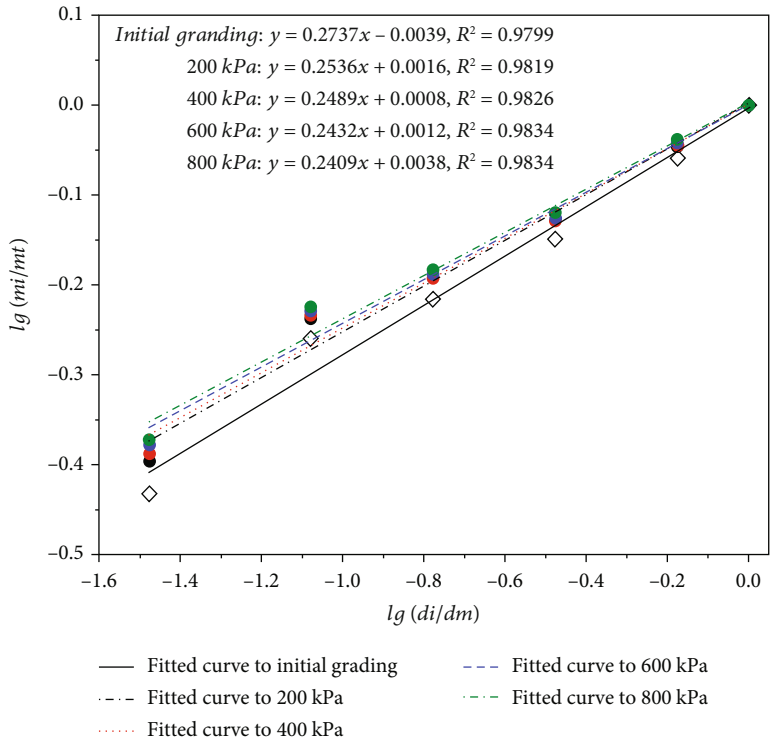

(b)

Figure 10: Continued.

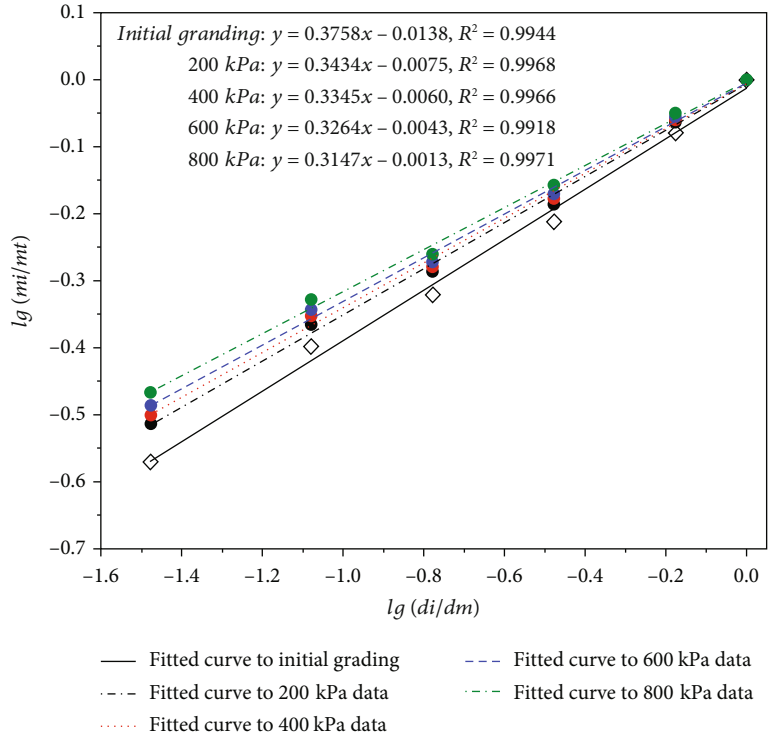

(c)

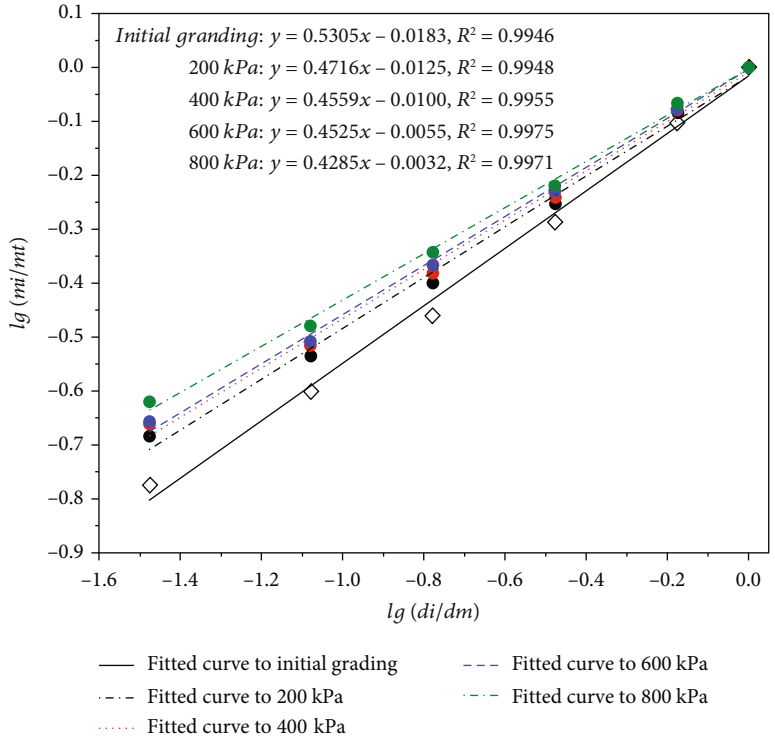

(d)

Figure 10: Fractal distribution curves of coarse-grained soils with different gradations before and after triaxial compression tests: (a) P_5 = 30%, (b) P_5 = 45%, (c) P_5 = 60%, and (d) P_5 = 75%.

Table 4: Statistical results of coarse-grained soil particle size fractal dimension before and after triaxial compression tests.

P_5 (%)	σ_3 (kPa)	Fractal dimension D		$\Delta D = D_2 - D_1$
		Before the tests D_1	After the tests D_2	
30	200	2.8019	2.8112	0.0093
	400	2.8019	2.8151	0.0132
	600	2.8019	2.8170	0.0151
	800	2.8019	2.8207	0.0188
45	200	2.7263	2.7464	0.0201
	400	2.7263	2.7511	0.0248
	600	2.7263	2.7568	0.0305
	800	2.7263	2.7591	0.0328
60	200	2.6242	2.6566	0.0324
	400	2.6242	2.6655	0.0413
	600	2.6242	2.6736	0.0494
	800	2.6242	2.6853	0.0611
75	200	2.4695	2.5284	0.0589
	400	2.4695	2.5441	0.0746
	600	2.4695	2.5475	0.0780
	800	2.4695	2.5715	0.1020

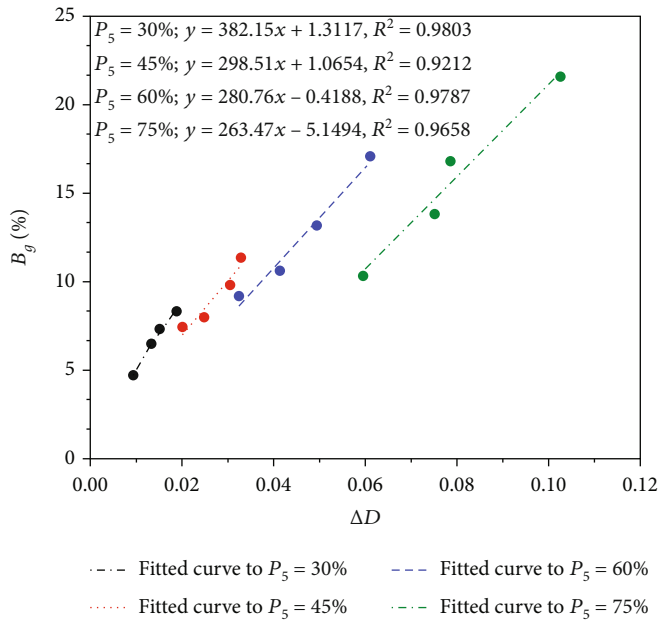

Figure 11: Relationship between particle breakage rate and fractal dimension difference.

mechanical properties of coarse-grained soils and play a controlling role in the shear deformation of soil. The mechanisms by which the coarse grain content and confining pressure affect the strength and deformation of the soil are discussed separately next.

5.1. Mechanisms Influencing the Strength of Coarse-Grained Soils. Coarse-grained soil consists of soil particles of different grain sizes; the squeezing each other, interlocking, and friction between particles constitute the shear strength of soil. However, the different arrangements and contact forms between the soil particles form different soil skeletal structures, which correspond to differ in their ability to resist external loads, as shown in Figure 13.

As can be seen from Figure 13(a), when the coarse grain content in the soil is less than 30%, the coarse particles are suspended in the fine particles, and the soil presents the structure of coarse-grained suspension. The fine particles are the substrate, and the coarse particles are the filling. The action between the coarse particles under load is weak, and the strength of the soil is mainly determined by the cohesive action of the fine particles. As can be seen from

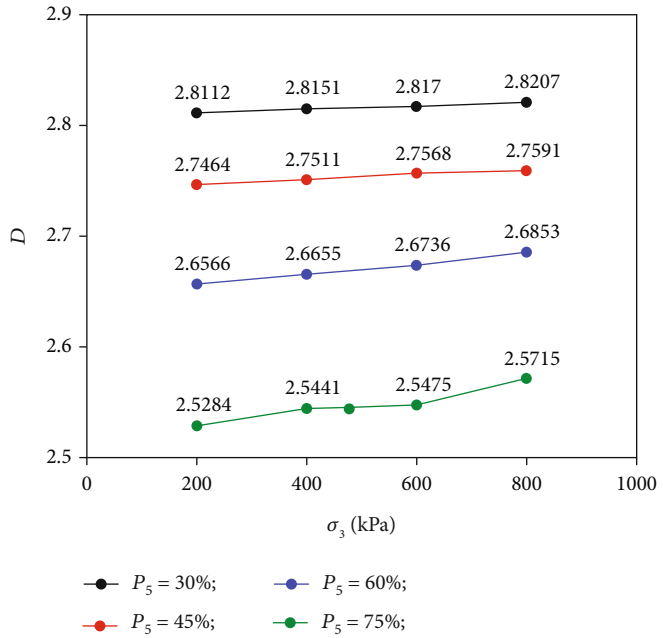

Figure 12: Relationship between particle size fractal dimension and confining pressure.

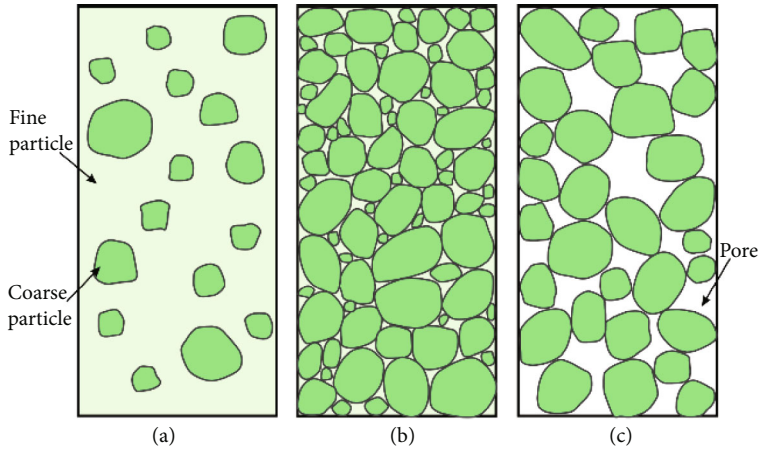

Figure 13: Contact structure of coarse particles: (a) coarse-grained suspension; (b) coarse-grained interlock; (c) coarse-grained overhead.

Figure 13(b), when the coarse grain content in the soil is 45%-60%, the coarse particles are mostly point-point contact or face-face contact, the fine particles are filled in the pores between the coarse particles, and the soil presents the structure of coarse-grained interlock. During the shear deformation process, the coarse particles roll and move, and soil particles are gradually squeezed and compacted. The external load is mainly borne by the skeletal structure formed by the coarse particles. As can be seen from Figure 13(c), when the coarse grain content in the soil is greater than 75%, the pores formed between the coarse particles gradually increase, and the fine particles cannot completely fill the pores, and the soil presents the structure of coarse-grained overhead. The shear strength of coarse-grained soil is mainly constituted by the occlusion and friction between coarse particles, coupled with the influence of stress concentration, the coarse particles break significantly, and the bearing characteristics of the soil body are very unstable.

5.2. Mechanisms Influencing the Deformation of Coarse-Grained Soils. The deformation of coarse-grained soils depends mainly on the relative movement between the internal particles and the degree of particle breakage. As the coarse grain content in the soil increases, the number of particles that interlock gradually increases. When the surrounding pressure is small and insufficient to limit the rolling and friction between the particles, the pore space of the particles gradually increases and the soil is deformed by negative dilatancy. On the other hand, when the coarse grain content in the soil and the confining pressure are both large, the particle breakage is more likely to occur due to the influence of the mutual squeezing and stress concentration among the

particles, while the rolling and movement of the particles are difficult to occur. As the fine particles formed by breakage gradually fill the pores of the coarse particles, the pore space of the soil decreases and positive dilatancy of the soil occurs.

6. Conclusions

Four groups of coarse-grained soil samples with different coarse-grained contents were prepared, and consolidated drained triaxial compression tests were carried out. Based on the experimental data, the shear deformation characteristics and particle breakage effects of soil mass were analyzed. The test results and conclusions are as follows:

(1) Coarse-grained soils with different coarse grain contents undergo negative dilatancy before positive dilatancy under the condition of low confining pressures. However, soil mass only shows the characteristics of positive dilatancy under the condition of high confining pressures. Confining pressure is an important factor affecting the dilatancy characteristics of coarse-grained soil, and lower confining pressures lead to more significant dilatancy

(2) With the increase of coarse grain contents, the structural characteristics of coarse-grained soil change, the occlusion and rolling between the block stone particles are intensified, and the positive dilatancy of soil is more obvious

(3) Applicability of quadratic function between axial strain ${\varepsilon_1}^2$ and lateral strain ε_3 is convinced for coarse-grained soil, and an experiential dilatancy criterion of coarse-grained soil considering confining pressure is established. The parameter $L = 4$ in the equation could serve as a criterion for whether the coarse-grained soil underwent positive dilatancy

(4) There are three kinds of particle breakage phenomena in shear deformation of coarse-grained soil: abrasion, attrition, and fracture. Particle breakage rate increases significantly with the increase of confining pressure and coarse grain contents. The degree of soil particle breakage can be characterized by the soil particle size fractal dimension differences before and after the test. The particle breakage rate increased significantly with the larger difference

(5) Due to the limitation of the testing machine, the confining pressure of triaxial compression test is less than 1 MPa, and the maximum particle size of soil is 60 mm in this study. The test phenomenon cannot fully reflect the mechanical properties of coarse-grained soils for dam construction. In order to fully reveal the shear deformation characteristics of coarse-grained soils, it is necessary to carry out mechanical tests of high confining pressure and full-scale model

Data Availability

The data used to support the findings of this study are included within the article.

Conflicts of Interest

The authors declare that they have no conflict of interest to this work.

Acknowledgments

This work was supported by the Special Basic Cooperative Research Programs of Yunnan Provincial Undergraduate University's Association (202001BA070001-066 and 202101BA070001-137), Basic Research Project of Yunnan Province of China (202101AT070144), and Talent Introduction Program of Kunming University (XJ20220015).

References

[1] Z. L. Cheng and J. J. Pan, "Some innovations and developments in the field of earth-rock dam engineering," *Journal of Yangtze River Scientific Research Institute*, vol. 38, no. 5, pp. 1–10, 2021.

[2] W. J. Xu and H. Y. Zhang, "Research on the effect of rock content and sample size on the strength behavior of soil-rock mixture," *Bulletin of Engineering Geology and the Environment*, vol. 80, no. 3, pp. 2715–2726, 2021.

[3] V. Andjelkovic, N. Pavlovic, Z. Lazarevic, and S. Radovanovic, "Modelling of shear strength of rockfills used for the construction of rockfill dams," *Soils and Foundations*, vol. 58, no. 4, pp. 881–893, 2018.

[4] J. J. Pan, J. W. Jiang, Z. L. Cheng, H. Xu, and Y. Z. Zuo, "Large-scale true triaxial test on stress-strain and strength properties of rockfill," *International Journal of Geomechanics*, vol. 20, no. 1, article 04019146, 2020.

[5] Y. Xue, J. Liu, P. G. Ranjith, F. Gao, H. P. Xie, and J. Wang, "Changes in microstructure and mechanical properties of low-permeability coal induced by pulsating nitrogen fatigue fracturing tests," *Rock Mechanics and Rock Engineering*, vol. 55, no. 12, pp. 7469–7488, 2022.

[6] D. Kim and S. Ha, "Effects of particle size on the shear behavior of coarse-grained soils reinforced with geogrid," *Materials*, vol. 7, no. 2, pp. 963–979, 2014.

[7] H. Y. Zhang, W. J. Xu, and Y.-Z. Yu, "Triaxial tests of soil-rock mixtures with different rock block distributions," *Soils and Foundations*, vol. 56, no. 1, pp. 44–56, 2016.

[8] Y. Wang, X. Li, J. M. He, Y.-F. Wu, and Y.-S. Wu, "Research status and prospect of rock and soil aggregate," *Journal of Engineering Geology*, vol. 22, no. 1, pp. 112–123, 2014.

[9] A. Tsomokos and V. N. Georginnou, "Effect of grain shape and angularity on the undrained response of fine sands," *Canadian Geotechnical Journal*, vol. 47, no. 5, pp. 539–551, 2010.

[10] J. G. Xia, R. L. Hu, S. W. Qi, W. Gao, and H. Y. Sui, "Large-scale triaxial shear testing of soil rock mixture containing oversized particles," *Chinese Journal of Rock Mechanics and Engineering*, vol. 36, no. 8, pp. 2031–2039, 2017.

[11] J. Wei, Y. F. Wei, and X. Huang, "A meso-scale study of the influence of particle shape on shear deformation of coarse-

grained soil," *Hydrogeology & Engineering geology*, vol. 48, no. 1, pp. 114–122, 2021.

[12] X. S. Shi, K. Liu, and J. H. Yin, "Effect of initial density, particle shape, and confining stress on the critical state behavior of weathered gap-graded granular soils," *Journal of Geotechnical and Geoenvironmental Engineering*, vol. 147, no. 2, article 04020160, 2020.

[13] N. P. Honkanadavar and K. G. Sharma, "Modeling the triaxial behavior of riverbed and blasted quarried rockfill materials using hardening soil model," *Journal of Rock Mechanics and Geotechnical Engineering*, vol. 8, no. 3, pp. 350–365, 2016.

[14] J. K. Liu, Q. M. Yu, J. Y. Liu, and D. Y. Wang, "Influence of non-uniform distribution of fine soil on mechanical properties of coarse-grained soil," *Chinese Journal of Geotechnical Engineering*, vol. 39, no. 2, pp. 562–572, 2017.

[15] S. S. Ahmed and A. Martinez, "Triaxial compression behavior of 3D printed and natural sands," *Granular Matter*, vol. 23, article 82, 2021.

[16] T. Sakai and M. Nakano, "Interpretation of the mechanical behavior of embankments having various compaction properties based on the soil skeleton structure," *Soils and Foundations*, vol. 55, no. 5, pp. 1069–1085, 2015.

[17] S. Zhu, Z. Y. Ning, C. X. Zhong, J. W. Chu, and Z. P. Gao, "Study on particle breakage and deformation characteristics of rockfill considering gradation effect," *Journal of Hydroelectric Engineering*, vol. 49, no. 7, pp. 849–857, 2018.

[18] W. L. Guo, Z. Y. Cai, Y. L. Wu, and Z. Z. Geng, "Estimations of three characteristic stress ratios for rockfill material considering particle breakage," *Acta Mechanica Solida Sinica*, vol. 32, no. 2, pp. 215–229, 2019.

[19] Y. L. Tu, H. J. Chai, X. R. Liu et al., "An experimental investigation on the particle breakage and strength properties of soil-rock mixture," *Arabian Journal of Geosciences*, vol. 14, no. 10, pp. 840–851, 2021.

[20] Y. Xiao, H. L. Liu, Q. S. Chen, L. H. Long, and J. Xiang, "Evolution of particle breakage and volumetric deformation of binary granular soils under impact load," *Granular Matter*, vol. 19, article 71, 2017.

[21] A. Simoni and G. T. Houlsby, "The direct shear strength and dilatancy of sand–gravel mixtures," *Geotechnical & Geological Engineering*, vol. 24, no. 3, pp. 523–549, 2006.

[22] B. X. Shi, S. C. Liu, X. L. Wu, and W. K. Chang, "Dilatancy behaviors of rockfill materials considering particle breakage," *Chinese Journal of Geotechnical Engineering*, vol. 43, no. 7, pp. 1360–1366, 2021.

[23] E. L. Wu, J. G. Zhu, S. B. He, and W. M. Peng, "A stress dilatancy relationship for coarse-grained soils incorporating particle breakage," *Granular Matter*, vol. 24, article 4, 2022.

[24] J. Y. Tang, D. S. Xu, and H. B. Liu, "Effect of gravel content on shear behavior of sand-gravel mixture," *Rock and Soil Mechanics*, vol. 39, no. 1, pp. 93–102, 2018.

[25] B. O. Hardin, "Crushing of soil particles," *Journal of Geotechnical Engineering*, vol. 111, no. 10, pp. 1177–1192, 1985.

[26] E. Alaei and A. Mahboubi, "A discrete model for simulating shear strength and deformation behaviour of rockfill material, considering the particle breakage phenomenon," *Granular Matter*, vol. 14, no. 6, pp. 707–717, 2012.

[27] M. Huang, Y. Yao, Z. Yin, E. Liu, and H. Lei, "An overview on elementary mechanical behaviors, constitutive modeling and failure criterion of soils," *China Civil Engineering Journal*, vol. 49, no. 7, pp. 9–35, 2016.

[28] M. C. Liu, F. Meng, and Y. Y. Wang, "Evolution of particle crushing of coarse-grained materials in large-scale triaxial tests," *Chinese Journal of Geotechnical Engineering*, vol. 42, no. 3, pp. 561–567, 2020.

[29] C. Wang, J. Y. Dong, Z. Q. Huang, J. J. Zhou, and J. H. Yang, "Effect of cobble content on the shear behaviour of sand-cobble mixtures," *Advances in Civil Engineering*, vol. 2021, Article ID 5554617, 9 pages, 2021.

[30] M. C. Liu, X. M. Huang, and Y. F. Gao, "Research on strength-deformation characteristics and nonlinear elastic model of rockfills," *Rock and Soil Mechanics*, vol. 25, no. 5, pp. 798–802, 2004.

[31] G. Zhang and J. M. Zhang, "Study on behavior of coarse-grained soil and its modeling," *Rock and Soil Mechanics*, vol. 25, no. 10, pp. 1587–1591, 2004.

[32] W. L. Xie, J. D. Wang, and L. H. Zhang, "Testing study on characteristics of strength and deformation for coarse materials," *Journal of Rock Mechanics and Engineering*, vol. 24, no. 3, pp. 430–437, 2005.

[33] R. J. Marsal, "Large scale testing of rockfill materials," *Journal of Soil Mechanics and Foundation Division*, vol. 93, no. 2, pp. 27–43, 1967.

[34] T. J. Zhang, J. W. Chen, R.-Y. Bao, X. K. Jiang, A. Zhou, and D. Ge, "Fractal characteristics of particle size distribution of crushed coal samples with different immersion time grading," *Journal of Mining and Safety Engineering*, vol. 35, no. 5, pp. 598–604, 2018.